JOURNAL OF CATALYSIS 155, 21–31 (1995)

Use of a Novel Temperature-Programmable Electrochemical Cell to Investigate Electrochemically Generated Surface Oxygen Species

R. T. Baker,* I. S. Metcalfe,*,[1] and P. H. Middleton†

*Department of Chemical Engineering and Chemical Technology and †Department of Materials, Imperial College of Science, Technology and Medicine, London, United Kingdom

Received September 7, 1994; revised January 23, 1995

A novel temperature-programmable electrochemical cell was designed and constructed. The cell consisted of a CaO-stabilised zirconia solid oxide electrolyte, an Ag cathode exposed to air, and an Ag, Au, or solid oxide anode. Electrochemical oxygen ion pumping (EOP) from the cathode could be performed in both constant-current and constant-potential-difference modes at a constant temperature or during a temperature programme. The gas exiting the anode chamber was analysed by a quadrupole mass spectrometer (QMS). During EOP, the O_2 detected by the QMS was found to be related faradaically to the charge passed across the electrolyte. Oxygen species formed on the anode surface during EOP were investigated by performing O_2 temperature-programmed desorption experiments with working anodes. Oxygen species derived electrochemically gave rise to a low-temperature desorption peak not seen for species formed from gaseous O_2. This electrochemically generated oxygen species may be related to the surface species postulated to be responsible for the non-faradaic electrochemical modification of catalytic activity effect (Vayenas, C. G., Bebelis, S., Yentekakis, I. V., and Lintz, H.-G., *Catal. Today* 11, 297 (1992)).

INTRODUCTION

Electrochemical oxygen ion pumping (EOP) is a technique by which a current of O^{2-} ions can be supplied to a working catalyst (1–12). A schematic diagram of a cell for EOP is shown in Fig. 1. A cell similar to a solid oxide fuel cell is employed. Electrochemically supplied oxygen is used only to modify the catalytic behaviour of the electrode of interest and is not the main supply of oxidant. It has been shown that oxygen supplied to an active electrode by EOP can have a significant effect on the activity and selectivity of a reaction (1–12). These effects are sometimes much greater than those seen if the extra oxygen were supplied as gas-phase O_2. This has led to proposals that different oxygen species may be formed, or that existing species may be altered, when oxygen is supplied electrochemically.

The NEMCA (non-faradaic electrochemical modification of catalytic activity) effect has been described as a reversible, electrochemically induced and controlled catalyst promotion effect (this effect has recently been reviewed in detail by Vayenas *et al.* (1)). Electrochemically generated oxygen species may spill over onto the metal surface, altering its work function. These species are not necessarily the reactive species but may act to promote other adsorbed species by altering the work function and so altering the surface–adsorbate bond strengths, favouring a particular reaction. X-ray photoelectron spectroscopy (XPS) (2, 7) and titration with ethene (1) have provided some evidence for such different electrochemically generated oxygen species on Ag electrodes.

Nagamoto *et al.* (8) compared the activity for oxidative coupling of CH_4 of electrochemically and gas-phase-supplied oxygen at about 750°C. EOP to the Ag electrode increased the production of both C_2's and CO_2 and gave rise to lower activation energies for both products. The activity of an Au electrode at 450°C with and without EOP was investigated by Hayakawa *et al.* (9). Under open circuit conditions and with O_2 present in the gas phase, the Au electrode was inactive for the oxidation of propene. However, when an O^{2-} current was supplied to the electrode, complete and partial oxidation products, including acrolein, were formed. The rate of acrolein production increased linearly with increasing current. This behaviour was observed with and without O_2 in the gas phase. Such results strongly suggested the electrochemical formation of a new oxygen species which was active for propene oxidation.

Temperature-programmed (TP) experiments are sensitive to the strength of surface–oxygen bonds, can be performed *in situ* at the high temperatures required for ionic conduction (unlike some other spectroscopic methods), and can be carried out in a time period comparable with the suggested relaxation time of the oxygen species (1).

[1] To whom correspondence should be addressed. E-mail: I.Metcalfe@ic.ac.uk.

0021-9517/95 $12.00

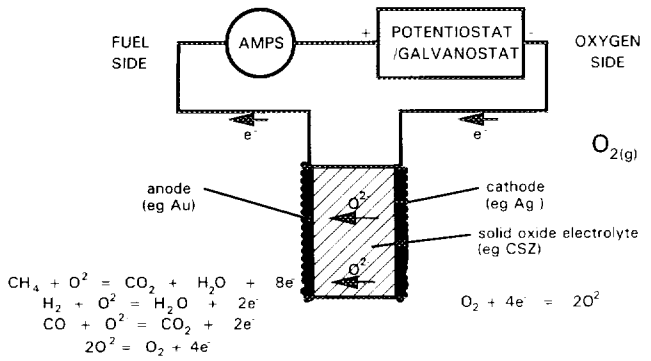

FIG. 1. Schematic diagram of apparatus required for electrochemical oxygen ion pumping.

Therefore, a temperature-programmable electrochemical cell would allow the investigation of the nature of such electrochemically generated surface oxygen species.

The aim of this work was to compare the behaviour of oxygen species formed by EOP with the behaviour of oxygen formed by adsorption from gas-phase O_2. An electrochemical cell capable of being temperature programmed was designed specifically for this work.

EXPERIMENTAL METHODS

A tubular design of temperature-programmable electrochemical reactor was chosen because of its overall simplicity and the easy availability of components. The use of two concentric tubes of carefully chosen diameters allowed the minimisation of system volume between the catalytic electrode and the detector. The system used allowed the seals to be made outside the furnace, away from the high temperatures and thermal cycling.

The overall configuration of the electrochemical cell is shown in Fig. 2. A vitreous CaO-stabilised zirconia (CSZ) tube of length 237 mm, outer diameter 6.35 mm (nominally 1/4") and wall thickness 0.82 mm (supplied by Zirconia Sales, Ltd.) was used as the electrolyte. The centre portion of the CSZ tube was enclosed inside a 3/8" (9.5 mm) quartz outer tube of internal diameter 7.2 to 7.5 mm and length 236 mm. The annulus between the two tubes formed the anode gas chamber. This was about 0.5 mm wide to minimise the volume of the anode chamber (2 to 2.5 ml) and the associated time delay during TP experiments. The anode was exposed to 100%He, 5%CH_4/He, or one of the pretreatment gases, 5%H_2/He or 20%O_2/He. 20%O_2/He was passed down the inside of the CSZ tube to supply the cathode. The temperature-programming system, flow system, and mass spectrometer detector are all described elsewhere (13). The mass spectrometer was calibrated daily for O_2, CO, CO_2, H_2O, H_2, and CH_4.

Ag, Au, $La_{0.8}Ca_{0.2}Cr_{0.9}Ni_{0.1}O_3$, and $La_{0.8}Ca_{0.2}Cr_{0.9}Co_{0.1}O_3$ anode materials were used. As the oxide materials were relatively poor electronic conductors, they were coated with a porous Au current collector. Ag and Au anodes were prepared by applying bands of the appropriate paint onto the CSZ tube and firing for 2 h at 800 and 980°C, respectively, after a slow temperature ramp. The oxides were applied as tape cast slurries which were prepared by a modified Pechini method (14) using nitrate precursors (15). Several coats of oxide slurry had to be applied and each was fired in air at 400°C for 2 then at 1350°C for 5 h for both $La_{0.8}Ca_{0.2}Cr_{0.9}Ni_{0.1}O_3$ and $La_{0.8}Ca_{0.2}Cr_{0.9}Co_{0.1}O_3$. An Au wire was wound around the oxide anode and bonded to it by painting on and firing the Au current collector. The wire was attached in the same way to the Ag anode using Ag paint. To keep the temperature gradient along the anode during temperature programming within acceptable limits, while presenting sufficient surface area to allow desorption and reaction products to be detected, the length of the anode in all cases was 10 mm.

The Ag cathode was formed on the inside surface of the CSZ tube along its whole length by sucking Ag paint into the tube using a pipette bulb, allowing the excess to drain out and temperature programming to 700°C. Ag electrical contacts were painted onto the lower end of the CSZ tube (Fig. 3). On assembly of the system, the stainless steel fittings were positioned so as to make electrical contact with these Ag bands.

The temperature was measured by a thermocouple inside the CSZ tube with its tip positioned at the level of

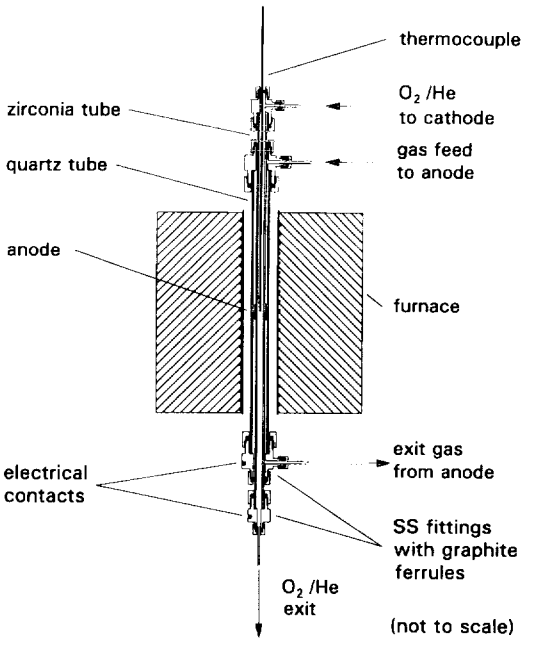

FIG. 2. The temperature-programmed electrochemical cell.

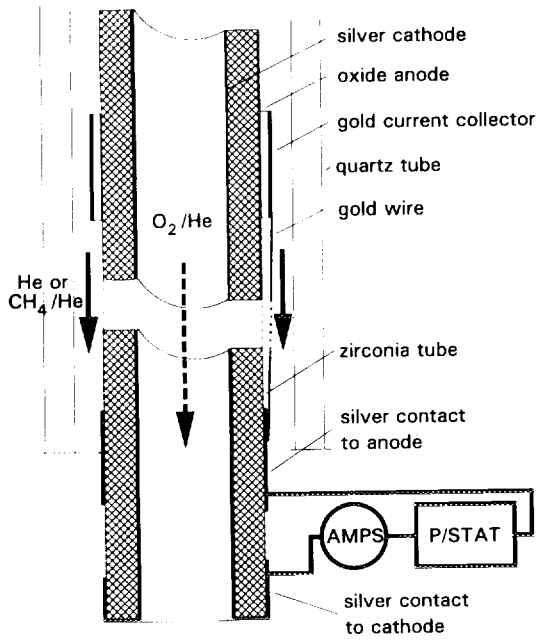

FIG. 3. Cell electrodes and electrical connections in the temperature-programmed electrochemical cell.

the anode. Any electrical interference caused by contact of the steel thermocouple sheath and the Ag cathode was prevented by placing a small ceramic bead on the thermocouple about 10 mm from the tip. A gas-tight glass sleeve was also used to isolate the thermocouple from its stainless steel fitting. The furnace temperature programmer was controlled by a thermocouple placed against the outside of the outer quartz tube at the level of the anode. Two electrically insulated clamps were used to support the system and hold it central in the furnace. A length of plastic tubing was included in the O_2/He line from the bottom stainless steel fitting to electrically isolate it and the cathode from the rest of the flow system. Temperature programmes were performed at heating rates of 25 or 50°C/min. The maximum temperature was limited to 900°C because of the melting point of the Ag cathode (962°C).

RESULTS

Electrochemical Oxygen Transport

To verify the faradaic behaviour of each anode system before further experiments, the temperature of the cell was increased in steps, a set potential was imposed at each temperature, and the steady state oxygen ion current and mass spectrometer O_2 response were recorded. These were then converted into equivalent moles of atomic oxygen using Faraday's constant or the mass spectrometer O_2 calibration, respectively, and were plotted against temperature. The effect of different potentials was also examined. These results gave an indication of how well the anodes had adhered to the CSZ tube and of the temperature and potential at which further experiments requiring significant amounts of electrochemically pumped O^{2-} could take place.

The results of these experiments were qualitatively similar for all anodes. The results obtained with an Ag electrode are presented in Fig. 4. There was generally good agreement between the number of moles of O^{2-} pumped to the anode and the increase in the number of moles of gas-phase O_2 (×2) detected by the quadrupole mass spectrometer (QMS). Initially, the oxygen ion current rose exponentially with increasing temperature, as expected for an activated conduction process. At high temperatures, however, the current tended towards a constant value as electrolyte resistance became negligibly small and the (constant) resistance of the external circuit became dominant. In Fig. 4, the electrochemical oxygen ion transport rate approached 5 μmol/min at 900°C when a pumping potential of 4.0 V was applied.

Temperature-Programmed Reaction Experiments

Temperature-programmed reaction (TPRx) experiments were performed with different anode systems using a 5%CH_4/He gas mixture. The heating rate was 25°C/min and flow rates were 55–60 ml/min for all experiments. Oxygen could be supplied to the electrode before the TPRx experiment either by gas-phase preoxidation in 20%O_2/He at 800°C for 1 h or by electrochemically "pre-pumping" O^{2-} ions. Alternatively, oxygen could be supplied during the TPRx experiment either by using a O_2/CH_4/He gas mixture or electrochemically by pumping O^{2-} ions at a constant potential difference or at a constant current.

TPRx experiments were performed on an Ag electrode and a $La_{0.8}Ca_{0.2}Cr_{0.9}Ni_{0.1}O_3$ electrode both with and without EOP during the experiment. An oxygen balance was

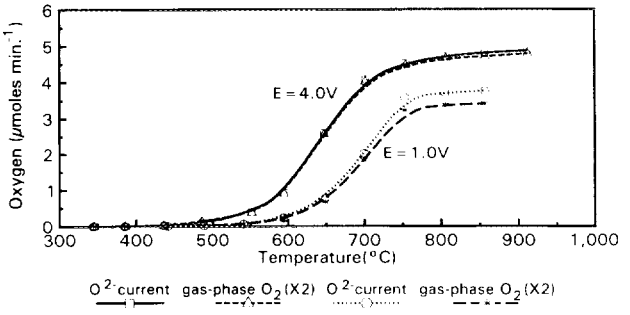

FIG. 4. Electrochemical oxygen pumping rate at different temperatures and potential differences as measured electrochemically and in the gas phase. Ag anode, CSZ electrolyte, Ag cathode.

then performed by subtracting the amount of oxygen detected in the gas-phase products formed without EOP from the amount of oxygen detected in the gas-phase products during EOP and comparing with the amount of oxygen supplied electrochemically. In all cases, a close agreement (<10–15% difference) between the amount of electrochemically supplied oxygen and the amount of extra oxygen detected in the gas phase was seen.

Temperature-Programmed Desorption (TPD) of Oxygen

TPD experiments were performed in order to investigate whether surface oxygen species supplied electrochemically to a catalytic anode material were different from those supplied by adsorption from the gas phase. Two anode systems were used, $La_{0.8}Ca_{0.2}Cr_{0.9}Co_{0.1}O_3$ with an Au current collector and Au alone. Both electrodes adhered well and sustained high currents. The experimental procedure was as follows.

(i) Several TPD cycles in 100%He were performed to desorb any contaminants from the surface.

(ii) Either

(a) electrochemical oxygen was supplied to the oxide anode at 500°C by imposing a potential of 3.0 V across the cell for 10 min. This gave an O^{2-} current of about 0.35 mA (1.09 μmol total). For the Au anode, a 3.0 V potential gave an O^{2-} current of 1.35 mA which was imposed for 3 min (1.26 μmol total) to provide approximately the same total moles of O^{2-} ions

or

(b) gas-phase oxygen was supplied at 500°C by injecting 2 × 500 μl pulses (8.2 μmol O_2) of 20%O_2/He into a stream of pure He passing through the anode chamber for the oxide anode. 3 × 500 μl pulses (12.3 μmol O_2) were injected for the Au anode.

(iii) The system was cooled to about 250°C by passing compressed air between the furnace and the outer quartz tube of the cell and any gas-phase O_2 was allowed to pass out of the system in the He flow. It was important that this step was carried out quickly to reduce the number of oxygen species which relaxed into other forms. A relaxation time constant of several minutes is quoted (1) for electrochemically generated oxygen ion species. About 4 min was the length of time required for this step of the experiment.

(iv) The temperature programme was started. The heating rates in the results presented here were all 50°C/min and the maximum temperature was typically 880°C.

(v) Steps (ii), (iii), and (iv) were repeated. (iia) and (iib) were generally alternated.

(vi) The mass spectrometer response to O_2 was calibrated.

Four blank O_2 TPD experiments were performed on the zirconia tube without an anode after exposure to 3 × 500 μl of O_2/He at 500°C. No desorption peaks were seen.

Figure 5 shows the O_2 traces for a set of consecutive TPD experiments on the $La_{0.8}Ca_{0.2}Cr_{0.9}Co_{0.1}O_3$/Au anode with alternating methods of oxygen supply. A clear, broad O_2 desorption peak was seen centred on 590°C in the experiments where oxygen was supplied electrochemically. No such peak was seen over that temperature range for the other traces where oxygen was adsorbed from the gas phase. However, a small peak (marked in Fig. 5) common to all traces appeared at around 720°C. Above 800°C a relatively very large oxygen desorption feature is seen in all cases. This can be attributed to the high temperature desorption of lattice oxygen from the $La_{0.8}Ca_{0.2}Cr_{0.9}Co_{0.1}O_3$ material. The electrochemically derived desorption peak at 590°C represented an average of 7.2×10^{-8} mol O_2 (equivalent to complete monolayer coverage over a surface area of 61 cm^2, assuming that an O_2 molecule occupies 0.141 nm^2 of the surface (16) whilst the peak at 720°C represented about 1.7×10^{-8} mol O_2 (equivalent to a monolayer area of about 15 cm^2). The total BET surface area of the $La_{0.8}Ca_{0.2}Cr_{0.9}Co_{0.1}O_3$/Au anode and the section of zirconia tube on which it was supported were measured, using Kr BET, as 38.9 cm^2. The geometric areas of the ends of the zirconia tube and the inner wall were subtracted (1.8 cm^2), giving a value of 37.1 cm^2.

Figure 6 shows the results of similar experiments using an Au anode. Again, a low-temperature peak (marked in Fig. 6) produced only by electrochemically supplied oxygen was seen centred on the lower temperature of about 510°C. The 510°C peaks averaged 4.20×10^{-8} mol O_2 (equivalent to complete coverage over about 36 cm^2). At about 710°C, a relatively sharp peak common to all traces was seen. This was much larger when the oxygen was supplied from the gas phase than electrochemically.

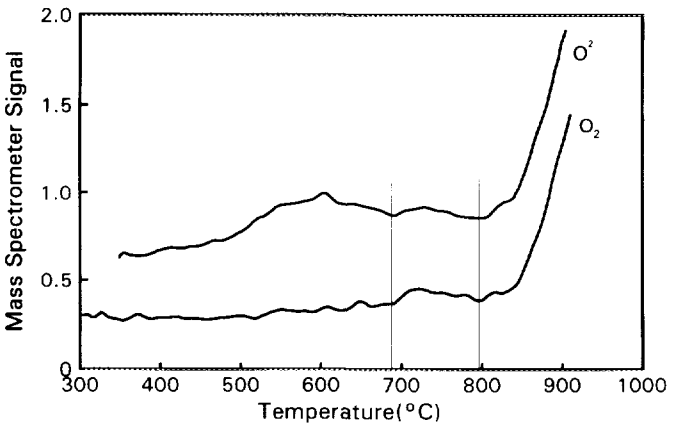

FIG. 5. O_2 TPD profiles from $La_{0.8}Ca_{0.2}Cr_{0.9}Co_{0.1}O_3$/Au electrode after adsorption of O_2 at 500°C or EOP at 500°C (O^{2-} denotes electrochemically pumped oxygen; O_2 denotes oxygen adsorbed from the gas phase). Parallel lines indicate the region in which the 720°C peak may be seen.

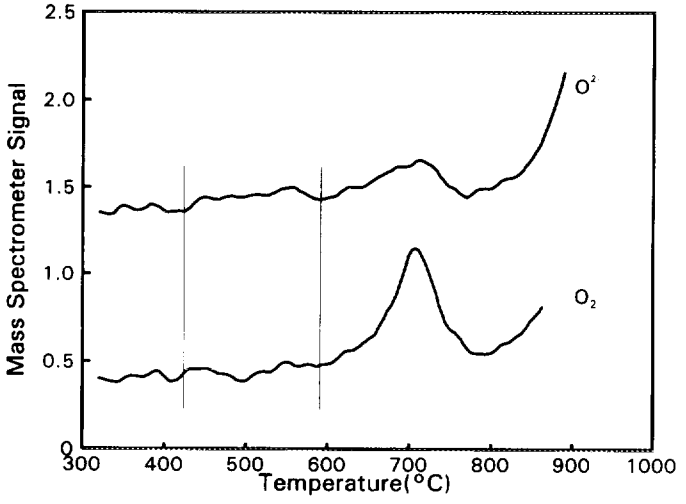

FIG. 6. O_2 TPD profiles from Au electrode after adsorption of O_2 at 500°C or EOP at 500°C (O^{2-} denotes electrochemically pumped oxygen; O_2 denotes oxygen adsorbed from the gas phase). Parallel lines indicate the region in which the 510°C peak may be seen on the O^{2-} spectrum.

The 710°C peak averaged 9.45×10^{-8} mol (about 80 cm^2) O_2 for gas-phase-supplied oxygen and 3.65×10^{-8} mol O_2 (31 cm^2) for electrochemically supplied oxygen. The BET surface area of the Au electrode was determined to be 124 cm^2. As in Fig. 5, above 800°C the O_2 appears in all cases, although it rose much less steeply for the Au anode. No oxide anode material was present so this feature cannot be attributed to the desorption of lattice oxygen in this case. The electrolyte material was not expected to give rise to oxygen desorption as none was seen in the blank experiments. One possible explanation is that differential thermal expansion at the seals of the system caused a small leak at these high temperatures, allowing a very small amount of O_2 to enter the anode chamber. It could also be possible for the residual electronic conductivity of the electrolyte at these high temperatures to result in oxygen transport across the membrane.

These TP experiments were performed several times and the results were found to be repeatable.

Scanning Electron Micrographs

Sections of tube supporting the $La_{0.8}Ca_{0.2}Cr_{0.9}Co_{0.1}O_3$/Au and the Au electrodes which had been used for the BET determination and a similar, blank section of zirconia tube were examined using scanning electron microscopy (SEM). SEM photographs were taken during this study and some of these are presented in Figs. 7a–7i. The electrolyte was seen to have relatively large grain sizes (Fig. 7a) of the order of 70 to 100 μm. This was as expected for a nominally vitreous material and implied that the surface area of the electrolyte is small compared to the surface areas of the Au and oxide layers and that it would, therefore, be unlikely to accommodate a significant amount of adsorbed species. Figures 7b and 7c show the structure of the oxide anode. The particles were highly uniform both in their spherical shape and in their size. They were also quite densely packed. The average particle diameter was measured from the photographs to be about 2.8 μm. The morphology of the Au current collector is shown in Figs. 7d and 7e. The Au layer appeared to consist of a porous network of fused spherical particles of significantly larger size (measured to be about 4.8 μm across) than the oxide particles. Figure 7f shows a cross section of the oxide material on the electrolyte and Fig. 7g shows the Au layer in cross section. The thicknesses of the oxide and the Au layers were about 10 and 3.3 μm, respectively. The volumes of the oxide anode and the Au current collector were calculated from these thicknesses and the geometric area of the anode. Using the average particle diameters given above and assuming spherical particles and cubic close packing, the number of particles and the total surface areas were estimated for the Au and the oxide layers. For the oxide anode, a value of 32 cm^2 was obtained. This value should be reasonably accurate since the oxide particles were densely packed and close to spherical, and occupied a narrow size range. A surface area of about 6 cm^2 was obtained for the Au. However, the spherical particles identified in the Au were fused and were less densely packed than in the oxide. Therefore, the true Au surface area can be expected to be less than this. The surface area of the zirconia directly beneath the anode would be expected to be close to the geometric surface area, 2 cm^2. These surface area values compare well with the value of 37 cm^2 obtained by BET determination.

SEM photographs were also taken of the Au anode in the Au–CSZ system. Figures 7h and 7i show the Au anode surface and edge, respectively. Comparison of Fig. 7h with Fig. 7d clearly shows that the Au anode had a much less well-defined structure than the Au current collector. No distinct particles could be identified and therefore it was not possible to make an estimate of the Au anode surface area, as was possible with the Au current collector. At 8 μm, the Au anode was much thicker than the Au current collector in the $La_{0.8}Ca_{0.2}Cr_{0.9}Co_{0.1}O_3$/Au/CSZ system (3.3 μm).

DISCUSSION

In the cases of both the $La_{0.8}Ca_{0.2}Cr_{0.9}Co_{0.1}O_3$/Au anode and the simple Au anode, an oxygen species was generated by electrochemical pumping of O^{2-} ions to the electrode which was not detected on exposure to gas-phase O_2 at the same temperature. These species desorbed in

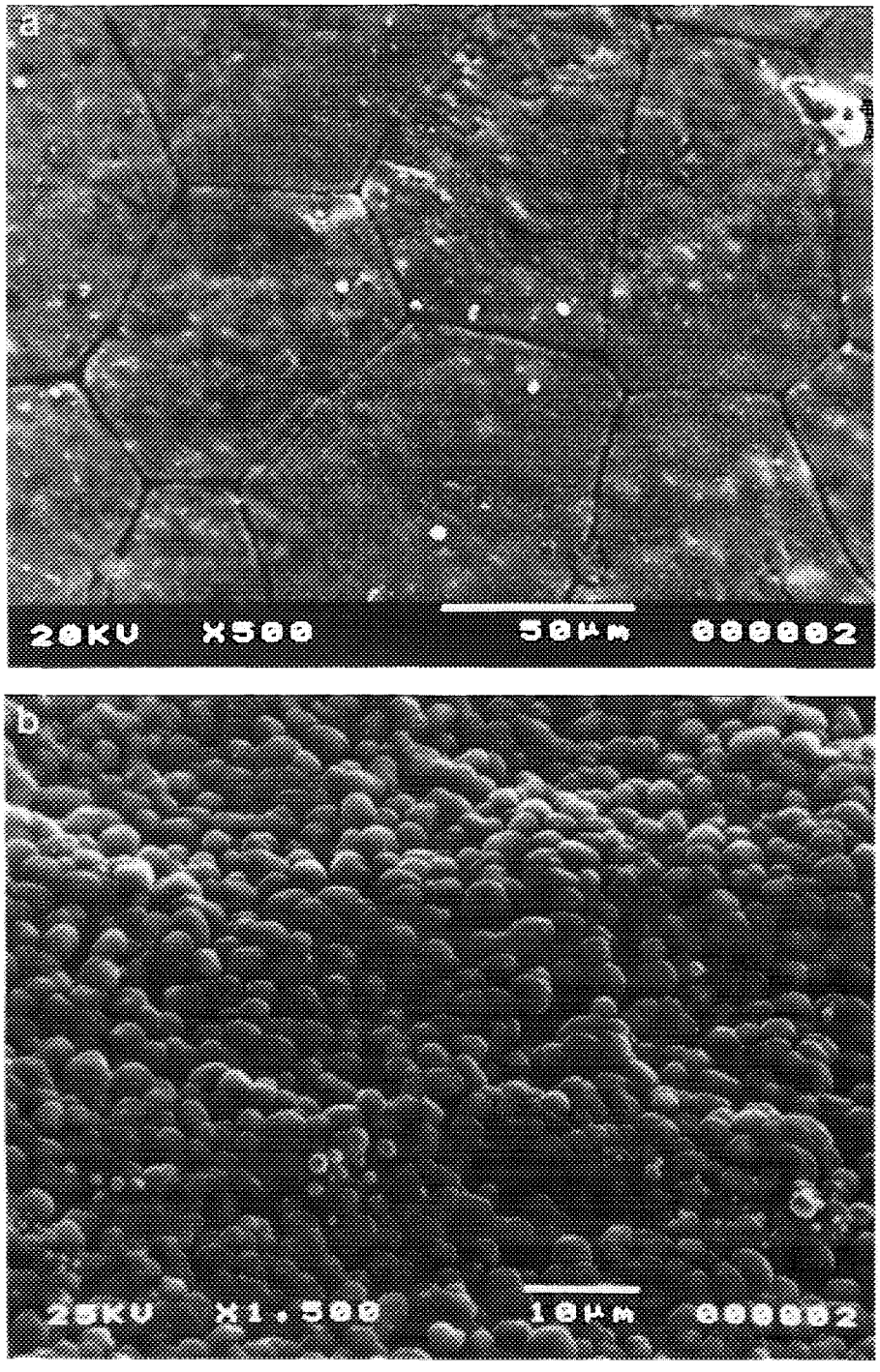

FIG. 7. SEM Photographs. (a) CSZ electrolyte; (b) and (c) $La_{0.8}Ca_{0.2}Cr_{0.9}Co_{0.1}O_3$ electrode; (d) and (e) Au current collector; (f) cross section of $La_{0.8}Ca_{0.2}Cr_{0.9}Co_{0.1}O_3$ anode on CSZ; (g) cross section of Au current collector on $La_{0.8}Ca_{0.2}Cr_{0.9}Co_{0.1}O_3$ anode; (h) Au electrode; (i) cross section of Au electrode.

the TPD experiments to give peaks centred at about 510°C and about 590°C for the Au only and the oxide/Au electrodes, respectively.

For the oxide/Au anode, this peak represented significantly more than a monolayer coverage of the whole anode surface. This suggested that the oxygen did not exist wholly on the anode surface. Since the amount of oxygen desorbed represented a surface coverage of ten times the measured surface area of the Au current collector and because oxygen is not generally believed to enter the Au bulk (see below), it is most likely that this oxygen was incorporated into the $La_{0.8}Ca_{0.2}Cr_{0.9}Co_{0.1}O_3$ (this may

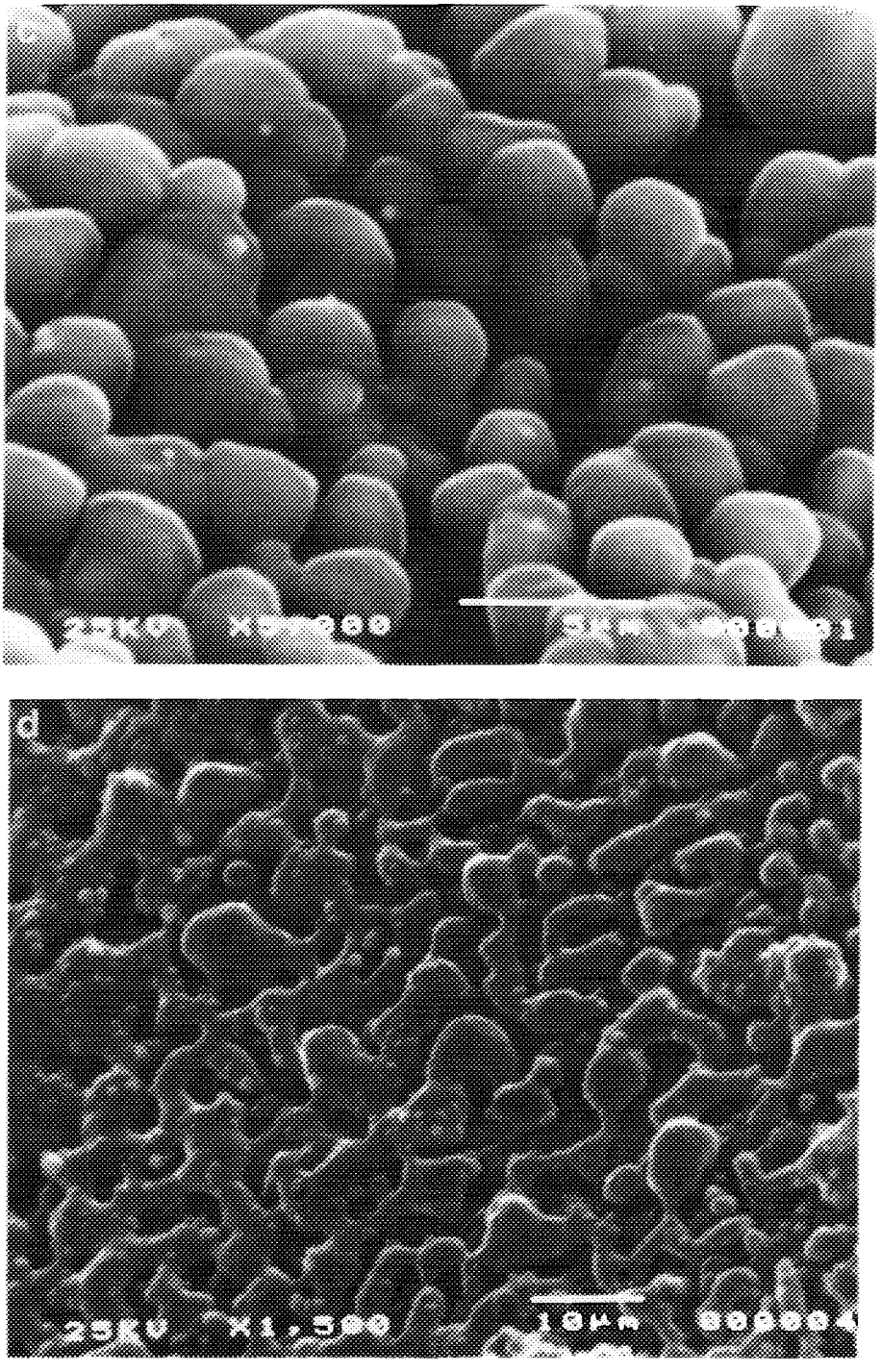

FIG. 7—*Continued*

have been in addition to the formation of an oxygen species on the surface of the Au). EOP may have caused a change in the nonstoichiometry at the surface of the oxide. Surface oxidative nonstoichiometry has been reported for $LaCrO_3$ in which the surface can achieve a composition of $LaCrO_{4.06}$ (17). This has been suggested to be caused by the presence of O^- ions at the oxide surface. It may be easier for these ions to be formed by EOP than through adsorption of O_2 at the same temperature. Such an explanation could be sufficient to account for the desorption of more than one surface monolayer equivalent of O_2.

The small, low-temperature oxygen desorption peak in Fig. 6 for the Au electrode was also seen only after EOP. This peak represented only 0.28 of a monolayer on the Au

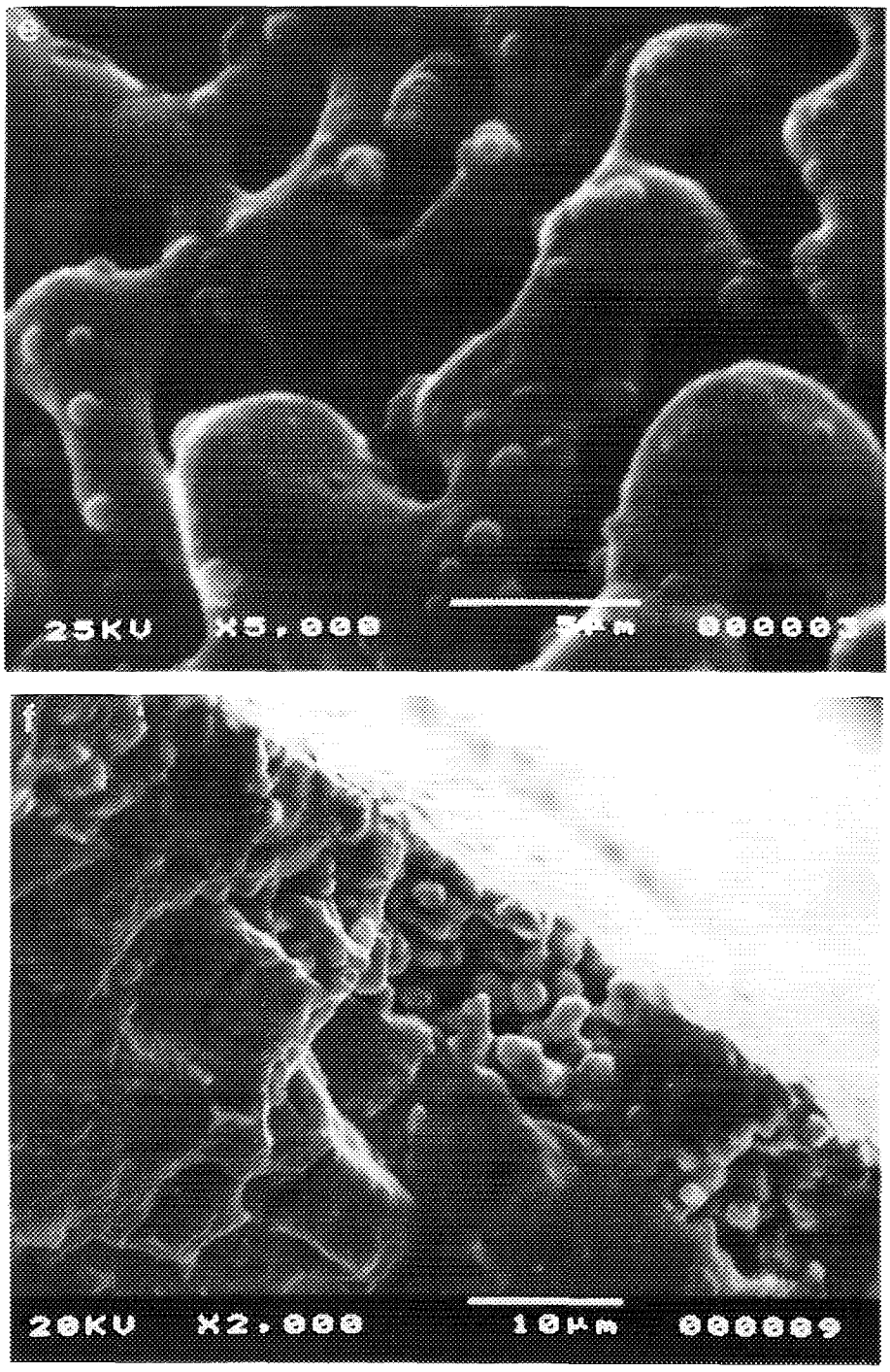

FIG. 7—*Continued*

surface and so could be attributed to an electrochemically generated chemisorbed oxygen species. Desorption of such a species from the Au current collector in the oxide/Au system (Fig. 5) would be masked by the desorption attributed to $La_{0.8}Ca_{0.2}Cr_{0.9}Co_{0.1}O_3$ above. It is interesting that Hayakawa *et al.* (9) proposed an electrochemically generated oxygen species on Au which was active for the oxidation of propene at 450°C. This is close to the temperature of 500°C at which EOP was conducted in the work presented here and is also lower than the temperature of desorption observed here. Therefore, it is possible that these two species are similar.

When oxygen was supplied either from the gas phase or by EOP to either anode type, an O_2 TPD peak was

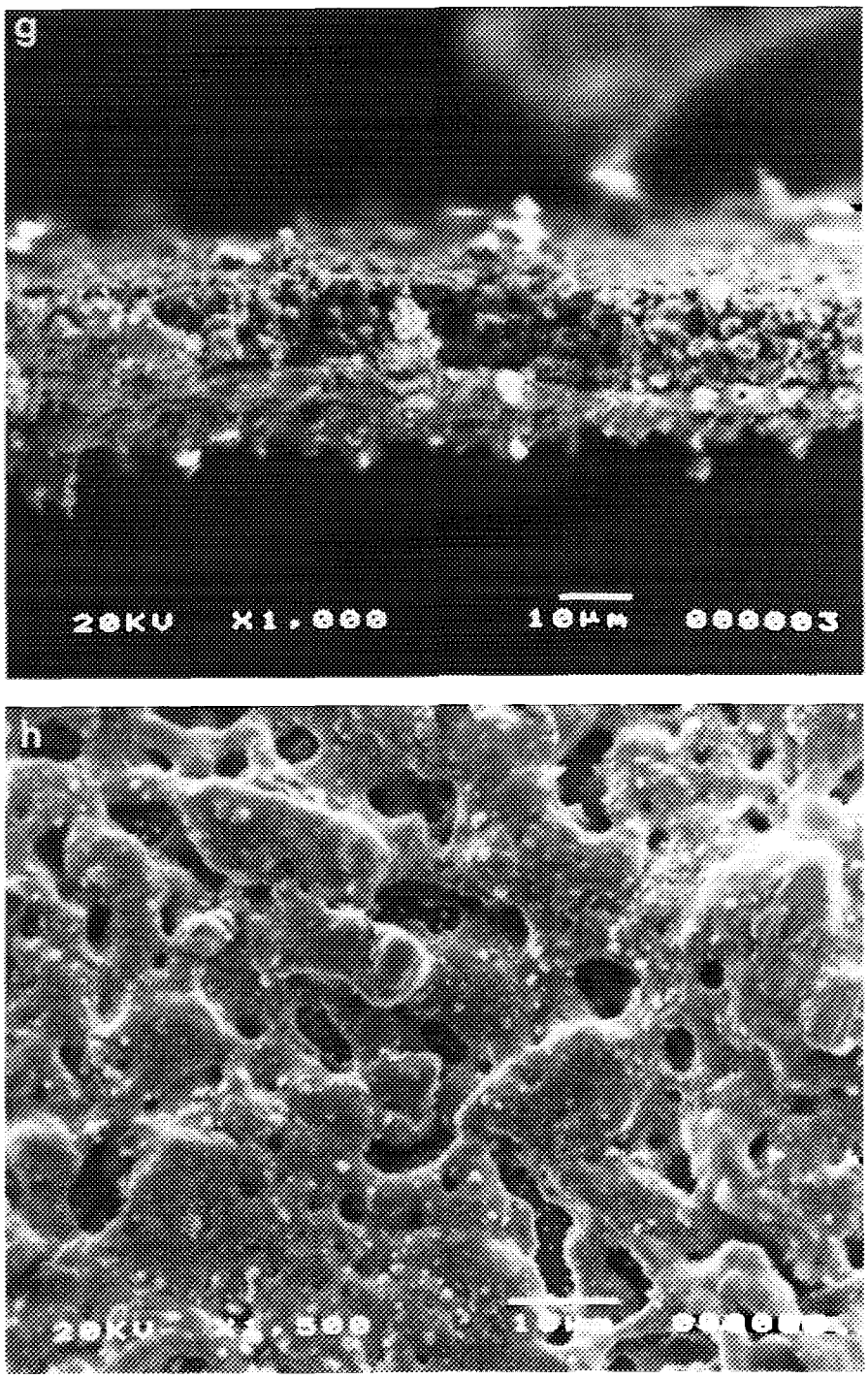

FIG. 7—*Continued*

seen at just above 700°C. This peak should be due to desorption from the Au surface, in the case of the Au electrode (in the case of the $La_{0.8}Ca_{0.2}Cr_{0.9}Co_{0.1}O_3$/Au electrode desorption from the oxide is also possible). The temperature seems high for the desorption of chemisorbed oxygen from a metal, particularly Au. Oxygen species on Au have been reported to be stable up to 800°C under vacuum (18). Such species could be caused by the formation of strong bonds with impurities in the Au, such as Ca and Si. This is a possibility in the work presented here since both the $La_{0.8}Ca_{0.2}Cr_{0.9}Co_{0.1}O_3$ and the CSZ contained Ca. The high temperatures involved in the preparation of the cell and during the experiments may have caused migration of impurities such as Ca into the Au.

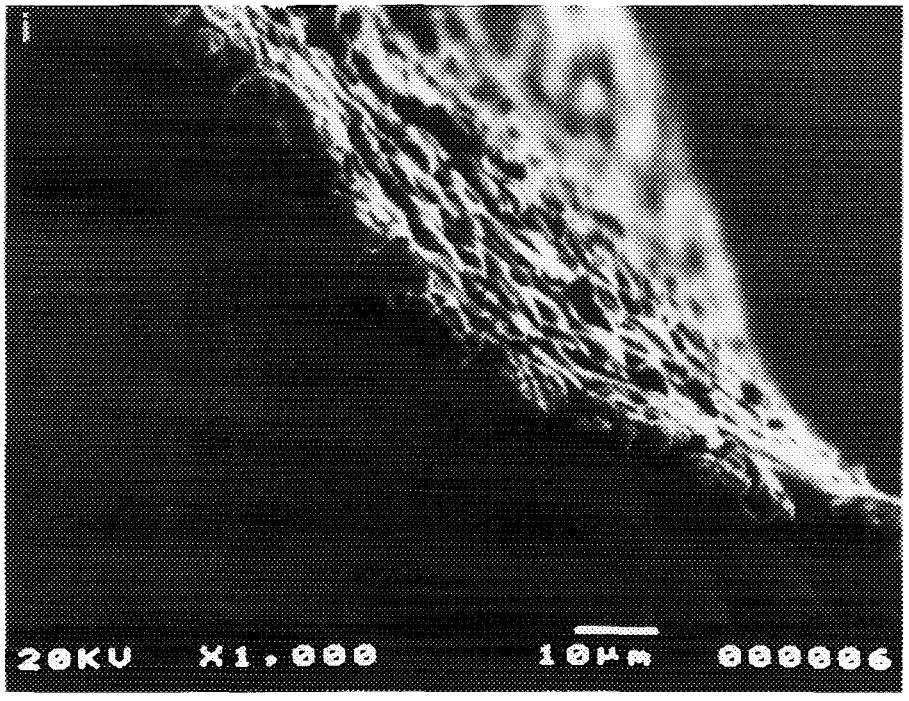

FIG. 7—*Continued*

It should be emphasised that the species responsible for the low-temperature oxygen desorption peak (510 and 590°C for Au only electrode and oxide/Au electrode, respectively) may also be present after exposure to gas-phase O_2, but in undetectable amounts. This could be due to differences in exposure conditions between the electrochemically and gas-phase-supplied oxygen. Consequently, the differences in the TPD profiles could be explained in terms of differences in exposure conditions, rather than in the activities of the electrode oxygen species, as discussed above. If this were the case, the profiles would be expected to have the same form but very different magnitudes. However, looking at Fig. 6, this is clearly not the case: while the high-temperature peak is clearly larger for gas-phase oxygen supply, the low temperature peak is detected only in the case of electrochemical oxygen supply. In addition, the samples were exposed to significantly more gas-phase O_2 than electrochemical O^{2-}.

CONCLUSIONS

A temperature-programmable electrochemical cell was designed and constructed. TPD and TPRx experiments on adsorbed and electrochemically generated oxygen species were performed. The cell was demonstrated to operate faradaically with both constant-current and constant-potential-difference O^{2-} ion pumping.

In O_2 TPD experiments, oxygen species were detected in the spectra for oxygen supplied to the electrode by EOP which were not detected when oxygen was adsorbed from the gas phase. With a $La_{0.8}Ca_{0.2}Cr_{0.9}Co_{0.1}O_3$/Au electrode, EOP appeared to cause the absorption of oxygen species into the $La_{0.8}Ca_{0.2}Cr_{0.9}Co_{0.1}O_3$ material. With an electrode of Au only, EOP gave rise to a TPD feature which was attributed to desorption of an electrochemically generated oxygen species from the Au surface. It seems likely that this Au surface oxygen species could be identified with the species active for propene oxidation in the work of Hayakawa *et al.* (9) and may be related to the surface species postulated by Vayenas *et al.* to be responsible for NEMCA (1).

ACKNOWLEDGMENTS

The authors thank the Science and Engineering Research Council and the Ceramic Electrochemical Reactor Club at Imperial College for financial support.

REFERENCES

1. Vayenas, C. G., Bebelis, S., Yentekakis, I. V., and Lintz H.-G., *Catal. Today*, **11**, 297 (1992).
2. Ladas, S., Kennou, S., Bebelis, S., and Vayenas, C. G., *J. Phys. Chem.* **97**, 8845 (1993).
3. Stoukides, M., and Vayenas, C. G., *J. Catal.* **70**, 137 (1981).
4. Tsiakaras, P., and Vayenas, C. G., *J. Catal.* **144**, 333 (1993).
5. Seimanides, S., and Stoukides, M., *J. Electrochem. Soc.* **133**, 1535 (1986).
6. Eng, D., and Stoukides, M., *J. Catal.* **130**, 306 (1991).

7. Arakawa, T., Saito, A., and Shiokawa, J., *Appl. Surf. Sci.* **16,** 365 (1983).
8. Nagamoto, H., Hayashi, K., and Inoue, H., *J. Catal.* **126,** 671 (1990).
9. Hayakawa, T., Tsunoda, T., Orita, H., Kameyama, T., Takahashi, H., Takehira, K., and Fukuda, K., *J. Chem. Soc. Chem. Comm.*, 961 (1986).
10. Otsuka, K., Yokayama, S., and Morikawa, A., *Chem. Lett.*, 319 (1985).
11. Otsuka, K., Suga, K., and Yamanaka, I., *Chem. Lett.*, 318 (1988).
12. Otsuka, K., Suga, K., and Yamanaka, I., *Catal. Lett.* **1,** 423 (1988).
13. Baker, R. T., Ph.D. thesis, University of London, 1994.
14. M. Pechini, U.S. Patent No. 3,330,697, July 1967.
15. G. M. Christie, Ph.D. thesis, University of London, 1987.
16. Kremenic, G., Nieto, J. M. L., Tascón, J. M. D., and Tejuca, L. J., *J. Chem. Soc. Faraday Trans. 1* **81,** 939 (1985).
17. Fierro, J. L. G., and Tejuca, L. G., *Appl. Surf. Sci.* **27,** 453 (1987).
18. Nguyen, N. V., Rincon-Rubio, L. M., and Mason, D. M., *J. Electrochem. Soc.* **133,** 1860 (1986).